Journal Pre-proof

Secondary scintillation yield from GEM electron avalanches in He-CF_4 and He-CF_4-isobutane for CYGNO — Directional Dark Matter search with an optical TPC

F.D. Amaro, E. Baracchini, L. Benussi, S. Bianco, C. Capoccia et al.

PII: S0370-2693(24)00317-4
DOI: https://doi.org/10.1016/j.physletb.2024.138759
Reference: PLB 138759

To appear in: *Physics Letters B*

Received date: 20 September 2023
Revised date: 24 May 2024
Accepted date: 24 May 2024

Please cite this article as: F.D. Amaro, E. Baracchini, L. Benussi et al., Secondary scintillation yield from GEM electron avalanches in He-CF_4 and He-CF_4-isobutane for CYGNO — Directional Dark Matter search with an optical TPC, *Physics Letters B*, 138759, doi: https://doi.org/10.1016/j.physletb.2024.138759.

This is a PDF file of an article that has undergone enhancements after acceptance, such as the addition of a cover page and metadata, and formatting for readability, but it is not yet the definitive version of record. This version will undergo additional copyediting, typesetting and review before it is published in its final form, but we are providing this version to give early visibility of the article. Please note that, during the production process, errors may be discovered which could affect the content, and all legal disclaimers that apply to the journal pertain.

© 2024 Published by Elsevier.

Journal Pre-proof

Secondary scintillation yield from GEM electron avalanches in He-CF_4 and He-CF_4-isobutane for CYGNO — Directional Dark Matter search with an optical TPC

F.D. Amaro[a], E. Baracchini[b,c], L. Benussi[d], S. Bianco[d], C. Capoccia[d], M. Caponero[d,e], D.S. Cardoso[f], G. Cavoto[g,h], A. Cortez[b,c], I.A. Costa[i,j], G. D'Imperio[h], E. Dané[d], G. Dho[b,c], F. Di Giambattista[b,c], E. Di Marco[h], F. Iacoangeli[h], H.P. Lima Júnior[k], G.S.P. Lopes[l], G. Maccarrone[d], R.D.P. Mano[a], R.R. Marcelo Gregorio[m], D.J.G. Marques[b,c], G. Mazzitelli[d], A.G. McLean[m], A. Messina[g,h], C.M.B. Monteiro[a,o], R.A. Nobrega[l], I.F. Pains[l], E. Paoletti[d], L. Passamonti[d], F. Petrucci[i,j], S. Piacentini[g,h], D. Piccolo[d], D. Pierluigi[d], D. Pinci[h], A. Prajapati[b,c], F. Renga[h], R.J.d.C. Roque[a,o], F. Rosatelli[d], A. Russo[d], G. Saviano[d,n], N.J.C. Spooner[m], R. Tesauro[d], S. Tomassini[d], S. Torelli[b,c], J.M.F. dos Santos[a]

[a] *LIBPhys, Department of Physics, University of Coimbra, 3004-516 Coimbra, Portugal*
[b] *Gran Sasso Science Institute, 67100, L'Aquila, Italy*
[c] *Istituto Nazionale di Fisica Nucleare, Laboratori Nazionali del Gran Sasso, 67100, Assergi, Italy*
[d] *Istituto Nazionale di Fisica Nucleare, Laboratori Nazionali di Frascati, 00044, Frascati, Italy*
[e] *ENEA Centro Ricerche Frascati, 00044, Frascati, Italy*
[f] *Centro Brasileiro de Pesquisas Fisicas, Rio de Janeiro 22290-180, RJ, Brazil*
[g] *Dipartimento di Fisica, Universitá La Sapienza di Roma, 00185, Roma, Italy*
[h] *Istituto Nazionale di Fisica Nucleare, Sezione di Roma, 00185, Rome, Italy*
[i] *Dipartimento di Matematica e Fisica, Universitá Roma TRE, 00146, Roma, Italy*
[j] *Istituto Nazionale di Fisica Nucleare, Sezione di Roma Tre, 00146, Rome, Italy*
[k] *Centro Brasileiro de Pesquisas Fisicas, Rio de Janeiro 22290-180, RJ, Brazil*
[l] *Universidade Federal de Juiz de Fora, Faculdade de Engenharia, 36036-900, Juiz de Fora, MG, Brasil*
[m] *Department of Physics and Astronomy, University of Sheffield, Sheffield, S3 7RH, UK*
[n] *Dipartimento di Ingegneria Chimica, Materiali e Ambiente, Sapienza Università di Roma, 00185, Roma, Italy*
[o] *Corresponding authors: cristinam@uc.pt, ritaroque@fis.uc.pt*

Abstract

CYGNO is an international collaboration with the aim of operating a 1 m^3 optical time projection chamber (TPC) for directional Dark Matter (DM) searches and solar neutrino spectroscopy, to be deployed at the Laboratori Nazionali del Gran Sasso (LNGS). A He/CF_4 (60/40) mixture is used, along with a triple Gas Electron Multiplier (GEM) cascade to amplify the ionization signal. The scintillation produced in the electron avalanches is read out using a scientific complementary metal–oxide–semiconductor (sCMOS) camera. This solution

Journal Pre-proof

Journal Pre-proof

has proven to provide very high sensitivity to interactions in the few keV energy range. The inclusion of a hydrogen-based gas will offer an even lighter target, resulting in a more efficient energy transfer in a DM particle collision, and consequently, a lower detection threshold. Additionally, longer track lengths of light nuclear recoils are easier to detect with a clearer direction. However, the addition of such gas will contribute to quenching the scintillation, jeopardizing the TPC performance. In this work, we demonstrate the feasibility of adding 1% to 5% isobutane to the He/CF_4 (60/40) mixture by measuring the respective absolute scintillation yield output. The overall scintillation produced in the charge avalanches is not drastically suppressed by quenching due to the isobutane addition. The presence of Penning transfer from excited He atoms to isobutane molecules increases the number of electrons in the avalanches, partially compensating for the loss of scintillation due to quenching. For the highest applied GEM voltage, the total number of photons produced in the avalanche per keV deposited in the absorption region presents a decrease of only a factor of about three, from $2.30(20) \times 10^4$ to $8.2(4) \times 10^3$ photons/keV, as the isobutane content increases from 0 to 5%. The quantification of the visible component of the scintillation shows that isobutane quenches both visible and ultraviolet (UV) photons emitted by He/CF_4.

Keywords: Secondary scintillation, Optical TPC, Rare event detection, Dark Matter, Directional Dark Matter, Neutrino, WIMP

1. Introduction

Dark matter (DM) search stands as one of the most important research areas in contemporary particle physics and cosmology, with Weakly Interacting Massive Particles (WIMPs) emerging as one of the most compelling candidates. Direct DM searches aim to detect nuclear recoils (NRs) resulting from WIMP elastic scattering in a sensitive volume of a radiation detector. Given the low rate and high background nature of these experiments, a main challenge lies in discriminating NRs due to WIMP scattering from interactions that produce electron recoils with significantly higher rates. Additionally, discriminating from NRs induced by neutrons interacting in the sensitive volume is an advantage. A detector with sensitivity to the direction of the incoming particle, reconstructing the 3D-topology of the respective ionization event [1, 2, 3, 4, 5, 6], offers a potential solution. This directional capability becomes crucial in the case of DM discovery, where the motion of the Earth and the Sun around the centre of the Galaxy generates, in the laboratory frame, an apparent wind of WIMPs coming from approximately the Cygnus constellation. This results in an anisotropic angular distribution of the WIMP-induced NRs, which, also due to the Earth's rotation, no background can mimic, providing a unique key for unambiguous and positive identification of DM signals [1]. Furthermore, the directional capability enables discrimination between WIMP scattering events and solar neutrino events that otherwise constitute an irreducible background

Journal Pre-proof

known as the "Neutrino Floor" [7], and allows to constrain DM halo models [1, 2, 3, 4, 5, 6].

CYGNO is part of a wider effort, the CYGNUS collaboration [2] that aims at developing instrumentation for directional DM searches. The CYGNO experiment [8, 9] focuses on developing a high-resolution optical Time Projection Chamber (TPC) for directional dark matter searches and solar neutrino spectroscopy. The ionization signal is amplified by a triple Gas Electron Multiplier (GEM) stack, with the secondary scintillation produced in the charge avalanches read out by suitable photosensors. Using 2D high-granularity scientific complementary metal–oxide–semiconductor (sCMOS) cameras in conjunction with fast light sensors, such as photomultiplier tubes (PMTs), for detecting the time profile of charge arrival at the amplification plane, enables the inference of the track extension along the drift direction and its inclination with respect to the amplification plane, faciliating the reconstruction of the 3D direction of the tracks [10, 11].

The TPC filling gas chosen is a He/CF_4 (60/40) mixture [12], providing high sensitivity to interactions in the few keV energy range together and excellent particle identification. This extends CYGNO's sensitivity to GeV and sub-GeV WIMP masses for spin-independent coupling and is suitable for atmospheric pressure operation while maintaining good tracking. Low mass nuclei result in longer track lengths, improving the determination of their direction, hence increasing directional sensitivity. CF_4 is added for its well-known scintillation in the visible region matching the sCMOS camera sensitivity. Additionally, fluorine provides sensitivity to spin-dependent WIMP-proton interactions.

The inclusion of a hydrogen-based gas offers an even lighter target, enhancing gas tracking capabilities in terms of drift velocity, diffusion, and longer track lengths [9]. The improvement in topological signature and particle identification of the recoil event enhances the rejection of natural radioactivity background down to low energy thresholds. Since the kinematic match between target and DM masses allows for better energy transfer to the recoiling nuclei, the addition of hydrogen will significantly improve the detectable capabilities for below 1 GeV DM candidates, Figure 1. More complete information on the foreseen CYGNO TPC sensitivity and its comparison with those of other experiments are shown in figures 14 and 15 of [9]. Hydrocarbons prove to be an excellent choice for additives to the base He/CF_4 mixture. However, the addition of such gas impacts the scintillation, reducing the amount of light detected during a recoil, which is a measurement of its energy, affecting the energy threshold of the experiment. The sCMOS camera is more affected due to its higher granularity and the higher level of scintillation required compared to PMTs. A higher energy threshold limits the detectable recoils, thereby reducing the DM sensitivity of the experiment. Previous studies demonstrated the energy threshold to be one of the most important experimental parameters for DM searches [13].

In this work, we present experimental studies of the absolute secondary scintillation yield produced in GEMs operated in a He/CF_4 (60/40) mixture and its admixture with a few percent of isobutane. We quantify this yield in terms of the total number of photons produced in GEM avalanches per keV

Journal Pre-proof

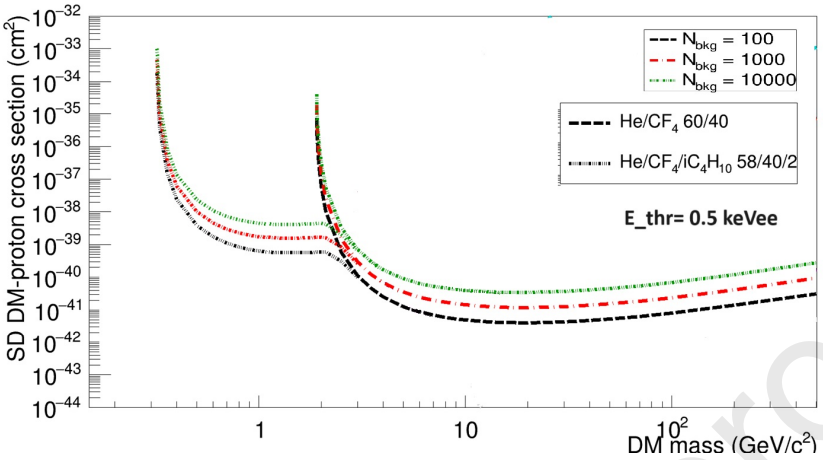

Figure 1: Spin-dependent sensitivity for WIMP–proton cross sections for the 30 m^3 CYGNO TPC with an operative threshold of 0.5 keV and for 3 years of exposure with different background level assumptions corresponding to different possible number of background events per year, N_{bkg} = 100 (black), 1000 (red) and 10,000 (dark green). The dashed curves show the sensitivity for a He/CF_4 (60/40) mixture, while the dotted curves show the sensitivity for a He/CF_4/isobutane (58/40/2) mixture.

deposited in the absorption region and/or per avalanche electron. The overall scintillation produced in the charge avalanches is not drastically suppressed by quenching due to the isobutane addition. The presence of the Penning transfer from excited He atoms to isobutane molecules increases the number of electrons in the avalanches, partially compensating for the loss of scintillation due to quenching

2. Experimental Setup

At present, CYGNO is operating a 50 L optical TPC prototype named LIME [9]. This prototype is currently collecting data underground at the Laboratori Nazionali del Gran Sasso (LNGS). The TPC operates in a 910 mbar He/CF_4 (60/40) mixture. For measuring the absolute scintillation yield of this mixture and its admixtures with isobutane, a dedicated setup was assembled for this purpose, as shown in Figure 2. An aluminium chamber of dimensions $23 \times 23 \times 5$ cm^3 was used to accommodate a drift mesh, a standard GEM foil, an induction mesh, and a Large Area Avalanche Photodiode (LAAPD). The GEM is a 50-µm thick Kapton foil coated on both sides with a 5-µm thick Cu film and perforated by biconical holes in a hexagonal pattern, with 70-µm and 50-µm diameter at Cu and Kapton, respectively. The meshes are made of stainless-steel wires, 80 µm in diameter, with 900-µm spacing, offering 84% optical transmission. The LAAPD is an Advanced Photonics Instruments, Deep-UV series, with a 16-mm diameter active area and spectral sensitivity in the 120–1000 nm range

Journal Pre-proof

[14], encompassing the entire emission spectrum of the He/CF_4 (60/40) mixture, between 200-800 nm [15], Figure 3. The visible component of the scintillation yield was also determined by placing a borosilicate glass filter, N-B270 [16], on top of the LAAPD to cut off photons below 300 nm, Figure 3. The sensitivity of the N-B270 is similar to that of the sCMOS camera: ORCA-Quest [17], Figure 3.

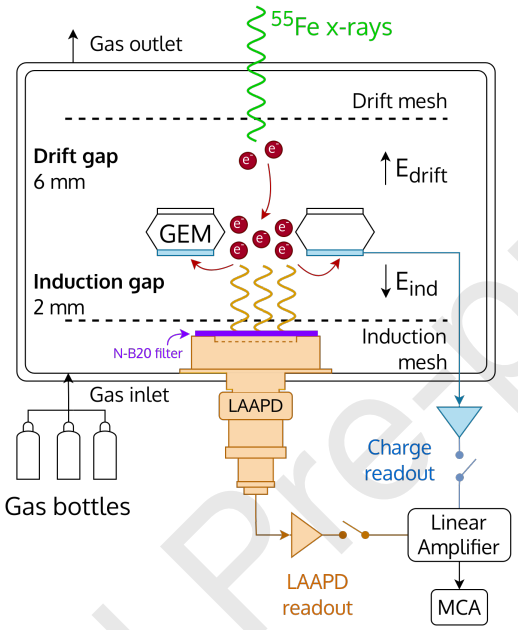

Figure 2: Schematic of the chamber used for the present studies.

Each electrode was individually biased with CAEN N471 modules, with current limited to 400 nA for the LAAPD and 100 nA for the remaining electrodes. Each power line was filtered using custom-made low pass filters with an RC constant of 20 ms to ensure stable biasing conditions and electronic noise filtering.

The chamber was operated in flow mode with a gas flow of about 4 $dm^3\,h^{-1}$. The uncertainty in concentrations is less than 0.025 %, 0.025 %, 0.25 %, in absolute value, for isobutane, CF_4 and He, respectively.

X-rays from a ^{55}Fe radioactive source, 2-mm collimated, were used. A fraction of the x-rays emitted by the source is absorbed in the gas in the drift region, and the resulting primary electrons are driven towards the GEM holes under the influence of a weak electric field, undergoing charge avalanche multiplication in the strong electric field inside the GEM holes. This electric field is induced by a voltage difference established between the GEM top and bottom electrodes, V_{GEM}. The avalanche electrons are collected and read out in the GEM bottom electrode, while the scintillation produced along the electron avalanches is read out by the LAAPD. Both output signals were amplified and formatted through

Journal Pre-proof

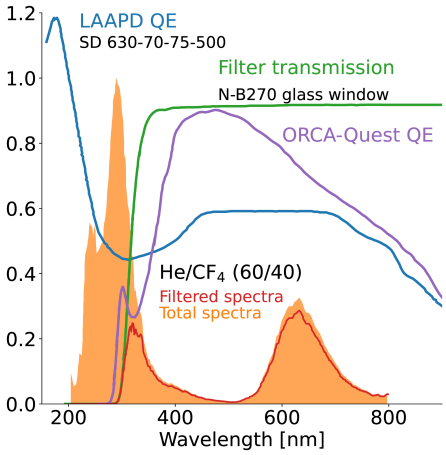

Figure 3: $He/CF_4(60/40)$ emission spectra (orange area), taken from [15], LAAPD quantum efficiency (blue), taken from [14]; Hamamatsu ORCA-Quest camera quantum efficiency (purple) [17] and N-B270 borosilicate glass filter transmission (green) [16]. The filtered spectra (red) was computed by multiplying the N-B270 filter transmission with the total emission spectrum of He/CF_4 (60/40).

typical preamplifier/amplifier elements, and their pulse height was analysed by a Multi-Channel Analyser (MCA).

The x-rays transmitted through the gas interact directly in the LAAPD. Therefore, a typical pulse-height distribution readout in the LAAPD comprises two main components, as shown in Figure 4 top panel: 1) the peak due to the direct x-ray interactions in the LAAPD, dependent only on the LAAPD biasing voltage,V_{APD}, and not on the voltages of the meshes or GEM electrodes; therefore, the channel corresponding to the position of this peak in the MCA is constant for a given V_{APD}; 2) the scintillation peak due to the photons produced in the avalanches in the GEM holes and impinging the LAAPD; its amplitude depends on V_{GEM} and the induction electric fields, for a given V_{APD}. A typical pulse-height distribution of the charge avalanche pulses read out at the GEM bottom electrode is depicted in Figure 4, bottom panel. Gaussian curves were fit to the peaks, from which the centroid and the full width at half maximum (FWHM) were extracted for average pulse amplitude and energy resolution measurements.

3. Methodology

The methodology used in this work closely follows the one previously described in earlier works [18, 19, 20]. The centroid channel in the MCA, A_X, of the peak corresponding to the peak resulting from direct interactions in the LAAPD enables direct calibration of the MCA channel number in terms of number of electron-hole pairs per channel, since the average energy needed to

Journal Pre-proof

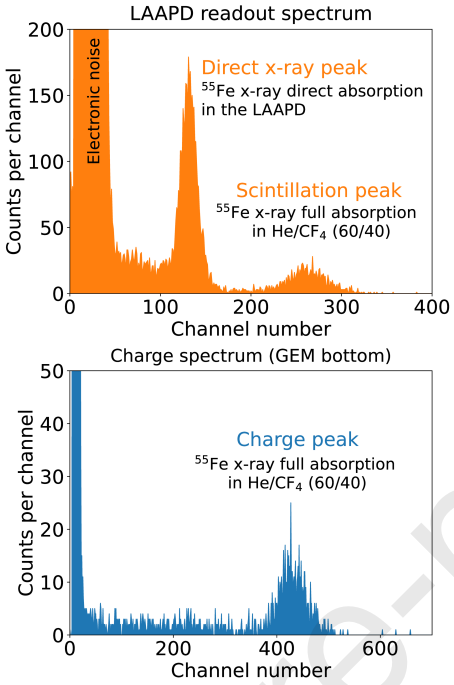

Figure 4: Typical pulse-height distributions obtained for x-rays from a ^{55}Fe radioactive source: (top) read out at the LAAPD output; (bottom) read out at the GEM bottom electrode; .

produce an electron-hole pair in Si, w(Si), due to 5.9-keV x-ray interactions is well known (3.62 eV [21]):

$$Cal_{Sc} = \frac{5.9\,\mathrm{keV}}{A_X \times w(\mathrm{Si})} \qquad \text{(electron-hole pairs/channel)} \tag{1}$$

Therefore, the number of electron-hole pairs produced in the LAAPD by the scintillation pulse, $N_{pe,Sc}$ is given by:

$$N_{pe,Sc} = A_{Sc} \times Cal_{Sc} = \frac{A_{Sc}}{A_X} \times \frac{5.9\,\mathrm{keV}}{w(\mathrm{Si})} \qquad \text{(electron-hole pairs)}, \tag{2}$$

where A_{Sc} is the centroid channel of the scintillation peak in the MCA.

The gain achieved in the scintillation amplification, G_{Sc}, i.e. the number of electron-hole pairs produced in the LAAPD per primary electron produced in the gas, is given by:

$$G_{Sc} = \frac{N_{pe,Sc}}{N_{pe,gas}} = \frac{A_{Sc}}{A_X} \times \frac{w(\mathrm{gas})}{w(\mathrm{Si})} \qquad \text{(electron-hole pairs/primary electron)}, \tag{3}$$

Journal Pre-proof

where w(gas) is the w-value of the gas mixture.

Finally, the secondary scintillation absolute yield, Y, i.e. the number of scintillation photons produced in the electron avalanches per primary electron created in the drift region, is determined as follows:

$$Y = \frac{A_{Sc}}{A_X} \times \frac{w(\text{gas})}{w(\text{Si})} \times \frac{1}{QE \times \Omega \times T} \qquad \text{(photons/primary electron)}, \tag{4}$$

where QE is the LAAPD average quantum efficiency, in electron-hole pairs per incident photon. It is obtained through the convolution of the LAAPD QE curve and the emission intensity distribution of He/CF_4 (60/40) as a function of photon wavelength [15] (54.0(27)%). Additionally, Ω is the relative solid angle subtended by the photodiode (0.224(11)) and T is the mesh transparency (84%, we consider the uncertainty in this parameter to be negligible).

Since the w-value of the He/CF_4 and He/CF_4+isobutane mixtures are not currently known to the best of our knowledge, in this work we define the secondary scintillation yield, Y/keV, as the number of photons produced in the electron avalanches per keV absorbed in the drift region,

$$Y/\text{keV} = \frac{N_{pe,Sc}}{5.9\,\text{keV}} \times \frac{1}{QE \times \Omega \times T} = \frac{A_{Sc}}{A_X} \times \frac{10^3}{w(\text{Si}) \times QE \times \Omega \times T} \quad \text{(photons/keV)}, \tag{5}$$

with w(Si) expressed in eV.

The number of avalanche electrons collected at the GEM bottom electrode is determined by the centroid channel of the respective peak after the MCA calibration in terms of electrons per channel, using a calibrated capacitor and a precise pulse generator (BNC PB-4 model).

4. Experimental Results and Discussion

To evaluate the performance of our setup, we performed measurements for the charge gain, defined as the number of electrons collected at the GEM bottom electrode per primary electron, as well as for the scintillation yield, Y, for pure CF_4 at atmospheric pressure. The results obtained with this setup are similar to previous results obtained in [22], thereby confirming the robustness and consistency of the results achieved with the current configuration.

The impact of the drift field intensity in He/CF4 (60/40) was accessed. Below $4\,\text{kV}\,\text{cm}^{-1}$, the drift field does not significantly affect the obtained avalanche charge gain, secondary scintillation yield and corresponding statistical fluctuations. Electric fields as low as $100\,\text{V}\,\text{cm}^{-1}$ can be applied without a substantial degradation of these parameters. Consequently, we used a drift field of $300\,\text{V}\,\text{cm}^{-1}$ in the subsequent studies.

Figure 5 depicts the experimental results for the total number of electrons produced in the avalanches within the GEM holes for He/CF_4 (60/40) + isobutane mixtures plotted against V_{GEM}. The data are presented for varying concentrations of 0, 1, 2, 3, 4, 5 and 10% isobutane, while keeping constant the ratio

Journal Pre-proof

between He and CF_4. The displayed data exhibit the characteristic logarithmic dependence of the charge on V_{GEM}, evident in the inserted graph within the main plot and depicted by the solid exponential trendlines. The charge growth factors, β, i.e. the coefficients of the exponential fit, for each isobutane content are provided in table 1.

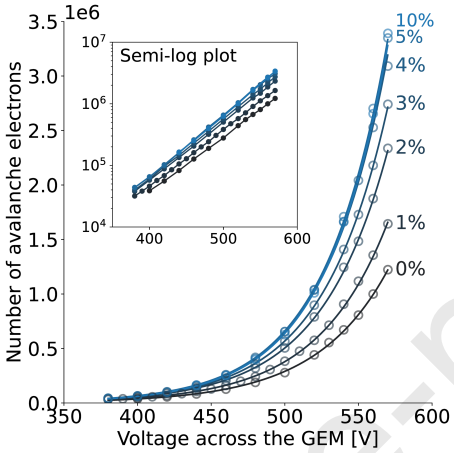

Figure 5: Total number of electrons produced in the avalanches in He/CF_4 (60/40) + isobutane mixtures as a function of GEM voltage for 0, 1, 2, 3, 4, 5 and 10% isobutane. The experimental measurements are presented by the open markers, whereas the corresponding exponential trendlines are presented by the solid lines. Error-bars are shown whenever uncertainties are larger than the maker-size.

The maximum voltage that can be applied across the GEM before the onset of micro-discharges, defined here as more than 1 discharge per minute, is independent of the isobutane concentration. The observed increase in the charge produced in the avalanches with increasing isobutane content can be attributed to the decrease of the gas w-value, which impacts on the GEM charge avalanche gain, and to the Penning transfer from excited He metastable states (19.8 eV and 20.6 eV [23]) produced in the avalanche to isobutane molecules (10.68(11) eV ionization energy [24]), resulting in additional electron-ion pair production. As the isobutane concentration increases, the fraction of excited He atoms escaping Penning effect decreases to zero, leading to saturation in the number of additional electrons produced by Penning effect, and subsequently, the number of avalanche electrons stabilizes. In fact, the total charge obtained for 10% isobutane content is comparable to that obtained for 5%, a factor of 3 higher than the total charge produced in He/CF_4 (60/40). At low V_{GEM} values, an increase in voltage results in larger gains and a lower avalanche fluctuation term, leading to a decrease in energy resolution. For higher values of V_{GEM}, the avalanche fluctuation term becomes less important and the energy resolution becomes constant. For higher V_{GEM} values, the achieved energy resolution for ^{55}Fe x-rays does not exhibit a significant dependence on the isobutane content, reaching

Journal Pre-proof

values around 14%.

Figure 6 shows the experimental results obtained for both the total and the visible component of secondary scintillation yield, Y/keV as a function of V_{GEM} for isobutane concentrations of 0, 1, 2, 3, 4 and 5%, in the top and bottom panel, respectively. Scintillation signals were also monitored for 10% isobutane, simultaneously with the charge signals, but the scintillation peak was not distinguishable under these conditions. As expected, for all mixtures, the secondary scintillation yield increases with increasing V_{GEM} following the exponential increase in the number of secondary electrons produced in the avalanche, as evidenced by the solid exponential trendlines. The scintillation growth factors, β, i.e. coefficients of the exponential fit, for each isobutane content are detailed in Table 1.

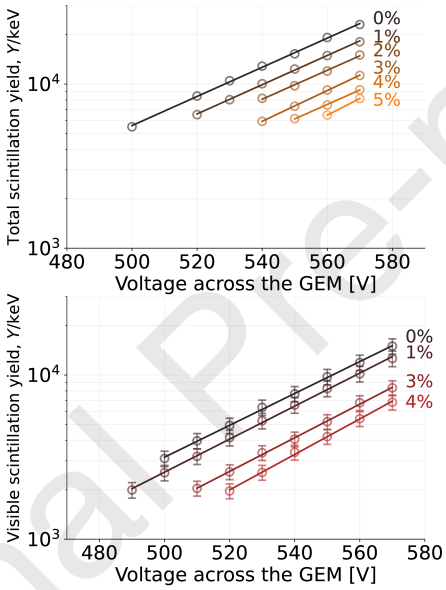

Figure 6: Total (top panel) and visible (bottom panel) secondary scintillation yield, Y/keV, produced in the GEM avalanches in He/CF_4 (60/40) + isobutane mixtures as a function of GEM voltage for 0, 1, 2, 3, 4 and 5% isobutane. The experimental measurements are depicted by the open markers, whereas the corresponding exponential trendline is presented by the solid lines. Error-bars are shown whenever uncertainties are larger than the maker-size.

Our results show that both the total and the visible component of the secondary scintillation yield decrease as the isobutane content increases. This decline is attributed to quenching by the isobutane molecules of the excited state species resulting from He and CF_4 excitation. In contrast, the energy resolution achievable at the highest values of V_{GEM} does not exhibit a significant dependence on the isobutane content, reaching values of about 20%. Our results align with those in [15], i.e. about 60% of the scintillation emitted by He/CF_4 (60/40) belongs to the visible component.

Journal Pre-proof

The secondary scintillation yield, expressed as the number of scintillation photons emitted per avalanche electron, Y/e^-, is depicted in Figure 7 as a function of V_{GEM} for the different isobutane concentrations under study. Notably, both the total (top panel) and visible (bottom panel) secondary scintillation yield per avalanche electron remain constant, independent of V_{GEM}. This observation implies that the number of photons emitted in an avalanche is proportional to the number of electrons produced in that same avalanche, and the ratio between total (overall) excitation and ionization cross-sections for electron impact is independent of the electric field intensity, for the electric field values corresponding to the range of applied GEM voltages. Figure 7 shows a decrease in the total and the visible secondary scintillation yields per avalanche electron with increasing isobutane concentration. The total number of photons produced in the avalanche is only 11.3(5) % of the total number of avalanche electrons in He/CF_4 (60/40), decreasing this value to 1.42(6) % for 5% of isobutane, Table 1. This is due to quenching, by the isobutane molecules, of the excited state species resulting from He and CF_4 excitations.

The average number of visible photons emitted per avalanche electron in He/CF_4 (60/40), as presented in Table 1, is consistent with the value found in the literature, which is 0.077(15) photons/avalanche electron [15]. Additionally, the average number of ultraviolet (UV) photons emitted per avalanche electron for the various isobutane admixtures was determined and is presented in Table 1. These values clearly indicate that isobutane quenches both the visible and the UV photons emitted by He/CF_4.

Table 1: Summary of the results obtained for He/CF_4 (60/40) + isobutane mixtures and for different isobutane contents.

% isobutane	0%	1%	2%	3%	4%	5%
Charge growth factor, β_C	0.02055(7)	0.02110(5)	0.02180(7)	0.02236(7)	0.02280(6)	0.02315(7)
Total scintillation growth factor, β_S	0.0204(12)	0.0205(17)	0.0203(32)	0.0216(32)	0.020(5)	0.023(10)
Visible scintillation growth factor, β_V	0.0223(16)	0.0232(14)	—	0.0236(20)	0.0249(25)	—
Total number of photons emitted per avalanche electron, Y/e^-	0.113(5)	0.0655(24)	0.0383(17)	0.0247(10)	0.0176(6)	0.0142(6)
Number of visible photons emitted per avalanche electron, Y/e^- (vis)	0.0669(27)	0.039(5)	—	0.0175(8)	0.0124(12)	—
Number of UV photons emitted per avalanche electron, Y/e^- (UV)	0.046(6)	0.027(6)	—	0.0072(13)	0.0052(13)	—

Despite the decrease by almost one order of magnitude in the total secondary scintillation yield per avalanche electron with an increase in isobutane concentration up to 5%, the secondary scintillation yield per keV deposited in the drift region only decreases by a factor of almost 3. While quenching diminishes the

Journal Pre-proof

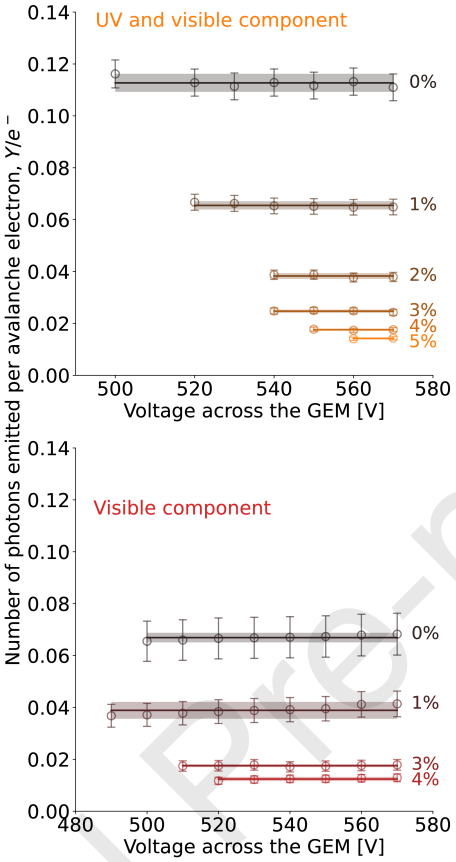

Figure 7: Total (top panel) and visible (bottom panel) secondary scintillation yield per avalanche electron, Y/e^-, produced in the GEM avalanches in He/CF_4 (60/40) + isobutane mixtures as a function of GEM voltage for 0, 1, 2, 3, 4 and 5% isobutane. The experimental measurements are depicted by the open markers. The average number of photons emitted per avalanche electron is presented by the horizontal solid line, whereas the corresponding coloured region illustrates their 95% confidence interval.

number of photons released per avalanche electron, the number of avalanche electrons increases due to the Penning effect and to the gas w-value decrease, partially compensating for the former effect.

Figure 8 shows the average percentage of the visible and the UV components of the scintillation emitted by the various He/CF_4 (60/40) + isobutane admixtures, calculated using the results from Figure 6 and Table 1. We observe that the UV component is more quenched with the addition of isobutane when compared to the visible component of the scintillation.

Journal Pre-proof

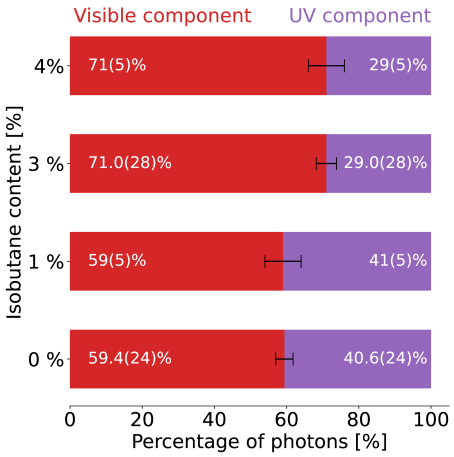

Figure 8: Percentage of the visible (red) and UV (purple) photons emitted by different isobutane admixtures to He/CF_4 (60/40). The error-bars correspond to a 95% confidence interval.

5. Conclusions

We studied the impact of adding isobutane to the He/CF_4 (60/40) mixture, specifically the production of charge and scintillation photons within electron avalanches occurring inside GEM holes. The studies involved measuring the total number of electrons produced in the avalanches, the number of both total and visible scintillation photons emitted in the avalanche per keV of energy absorbed in the drift region, and the number of photons emitted per avalanche electron. These measurements were performed as a function of the voltage across the GEM, V_{GEM}, considering isobutane concentrations of 0, 1, 2, 3, 4 and 5% added to the He/CF_4 (60/40) mixture.

While the number of photons produced in the avalanches per avalanche electron is reduced by 90% reduction as isobutane increases from 0 to 5%, due to quenching of the excited state species from He and CF_4 excitations, the overall scintillation produced in the charge avalanches only decreases by 35%. This reduction is attributed to the simultaneous presence of Penning transfer from He excited atoms to isobutane molecules and to the reduction in the gas w-value. This process increases the number of electrons in the avalanches with increasing isobutane content, thereby enhancing the photon output and partially compensating for the loss of scintillation due to quenching.

The maximum voltage applicable to the GEM was found to be independent of the isobutane concentration. The results exhibit a constant secondary scintillation yield per avalanche electron, independent of V_{GEM}, denoting a constant ratio between the total (overall) ionization and excitation cross sections for electron impact within the electric field intensity range corresponding to the studied GEM voltages. Additionally, the results demonstrate that isobutane quenches both the visible and the UV photons emitted by He/CF_4 (60/40), with a more

Journal Pre-proof

pronounced attenuation of the UV component. The visible component constitutes approximately 59.4(24)% of the total photon emission for He/CF_4 (60/40), increasing to about 71(5)% for isobutane concentrations around 4%.

Future studies will explore the potential to enhance the secondary scintillation yield by using a higher concentration of CF_4. Given that scintillation in these mixtures is generated through CF_4 a higher concentration may compensate for the decrease in yield caused by the addition of isobutane.

6. Acknowledgements

R.J.C. Roque acknowledges FCT PhD grant SFRH/BD/143355/2019; C.M.B. Monteiro acknowledges DOI:10.54499/CEECIND/04434/2017/CP1460/CT0027. Work supported by CERN/FIS-INS/0013/2021, CERN/FIS-TEC/0038/2021 (DOI:10.54499/CERN/FIS-TEC/0038/2021) and UIDB/FIS/04559/2020 (DOI: 10.54499/UIDB/04559/2020), funded by national funds through FCT/MCTES and co-financed by the European Regional Development Fund (ERDF) through the Portuguese Operational Program for Competitiveness and Internationalization, COMPETE 2020. Part of this project has received funding from the European Union's Horizon 2020 re-search and innovation programme from the European Research Council (ERC) grant agreement No 818744. This work is partially supported by ICSC — Centro Nazionale di Ricerca in High Performance Computing, Big Data and Quantum Computing, funded by European Union — NextGenerationEU.

References

[1] F. Mayet, A. M. Green, J. B. R. Battat, et al., A review of the discovery reach of directional Dark Matter detection, Phys. Rep. 627 (2016) 1–49.

[2] S. E. Vahsen, C. A. J. O'Hare, W. A. Lynch, et al., CYGNUS: Feasibility of a nuclear recoil observatory with directional sensitivity to dark matter and neutrinos, arXiv preprint arXiv:2008.12587 (2020).

[3] NEWSdm Collaboration, Directional Dark Matter Search with NEWSdm, Moscow University Physics Bulletin 77 (2) (2022) 284–287.

[4] Y. Hochberg, E. D. Kramer, N. Kurinsky, B. V. Lehmann, Directional detection of light dark matter in superconductors, Phys. Rev. D 107 (2023) 076015.

[5] A. Anokhina, V. Gulyaeva, E. Khalikov, et al., Directional Observation of Cold Dark Matter Particles (WIMP) in Light Target Experiments, Universe 7 (2021) 215.

[6] J. B. R. Battat, C. Eldridge, A. C. Ezeribe, et al., Improved sensitivity of the DRIFT-IId directional dark matter experiment using machine learning, JCAP 2021 (2021) 014.

Journal Pre-proof

[7] C. A. J. O'Hare, New definition of the neutrino floor for direct dark matter searches, Phys. Rev. Lett. 127 (2021) 251802.

[8] F. D. Amaro, E. Baracchini, L. Benussi, et al., Directional Dark Matter Searches with CYGNO, Particles 4 (2021) 343–353.

[9] F. D. Amaro, E. Baracchini, L. Benussi, et al., The CYGNO experiment, Instruments 6 (2022) 6.

[10] V. C. Antochi, E. Baracchini, G. Cavoto, et al., Combined readout of a triple-GEM detector, J. Instrum. 13 (2018) P05001.

[11] V. C. Antochi, E. Baracchini, L. Benussi, et al., Performance of an optically read out time projection chamber with ultra-relativistic electrons, Nucl. Instrum. Meth. A 999 (2021) 165209.

[12] E. Baracchini, L. Benussi, S. Bianco, et al., Stability and detection performance of a GEM-based Optical Readout TPC with He/CF_4 gas mixtures, J. Instrum. 15 (2020) P10001.

[13] A. M. Green, B. Morgan, Optimizing WIMP directional detectors, Astroparticle Physics 27 (2007) 142–149.

[14] Advanced Photonix, 1240 Avenida Acaso, Camarillo, CA 93012, Non-Cooled Large Area DUV Silicon Avalanche Photodiode SD 630-70-75-500, https://www.advancedphotonix.com/ (2024).

[15] M. M. F. R. Fraga, F. A. F. Fraga, S. T. G. Fetal, et al., The gem scintillation in He-CF_4, Ar-CF_4, Ar-TEA and Xe-TEA mixtures, Nucl. Instrum. Meth. A 504 (2003) 88–92.

[16] CRYSTRAN, Optical Glass (N-BK7 types), CRYSTRAN (2012).

[17] Hamamatsu, ORCA-Quest qCMOS camera C15550-20UP, Hamamatsu (2022).

[18] C. M. B. Monteiro, J. A. M. Lopes, J. F. C. A. Veloso, J. M. F. Dos Santos, Secondary scintillation yield in pure argon, Phys. Lett. B 668 (2008) 167–170.

[19] C. M. B. Monteiro, A. S. Conceicao, F. D. Amaro, et al., Secondary scintillation yield from gaseous micropattern electron multipliers in direct dark matter detection, Phys. Lett. B 677 (2009) 133–138.

[20] C. M. B. Monteiro, L. M. P. Fernandes, J. F. C. A. Veloso, C. A. B. Oliveira, J. M. F. Dos Santos, Secondary scintillation yield from GEM and THGEM gaseous electron multipliers for direct dark matter search, Phys. Lett. B 714 (2012) 18–23.

[21] G. F. Knoll, Radiation detection and measurement John Wiley & Sons, Vol. 65, John Wiley & Sons, 2000.

Journal Pre-proof

[22] H. N. da Luz, A. S. Conceicao, J. F. C. A. Veloso, et al., GEM Operation in High-Pressure CF_4: Studies of Charge and Scintillation Properties, IEEE Trans. Nucl. Sci. 56 (2009) 1564–1567.

[23] I. Korolov, M. Leimkühler, M. Boeke, et al., Helium metastable species generation in atmospheric pressure RF plasma jets driven by tailored voltage waveforms in mixtures of He and N_2, J. Phys. D. 53 (2020) 185201.

[24] S. G. Lias, Ionization Energy Evaluation, NIST Chemistry WebBook, NIST Standard Reference Database Number 69.

Journal Pre-proof

Journal Pre-proof

Declaration of interests

☒ The authors declare that they have no known competing financial interests or personal relationships that could have appeared to influence the work reported in this paper.

☐ The authors declare the following financial interests/personal relationships which may be considered as potential competing interests:

Journal Pre-proof